# Geophysical Research Letters®

**Key Points:**

- Increased insolation during austral summer due to orbital precession shifts the southern westerlies poleward
- Poleward shifted westerlies enhance $CO_2$ outgassing due to increased turbulent exchange and vertical transport of carbon-rich waters
- Enhanced transport of carbon-rich waters is driven by a deepening of the overturning circulation in response to poleward shifted winds

# The Impact of Orbital Precession on Air-Sea $CO_2$ Exchange in the Southern Ocean

Cole F. Persch[1] , Pedro DiNezio[1], and Nicole S. Lovenduski[1,2]

[1]Department of Atmospheric and Oceanic Sciences, University of Colorado, Boulder, Boulder, CO, USA, [2]Institute of Arctic and Alpine Research, University of Colorado, Boulder, Boulder, CO, USA

**Abstract** Orbital precession has been linked to glacial cycles and the atmospheric carbon dioxide ($CO_2$) concentration, yet the direct impact of precession on the carbon cycle is not well understood. We analyze output from an Earth system model configured under different orbital parameters to isolate the impact of precession on air-sea $CO_2$ flux in the Southern Ocean—a component of the global carbon cycle that is thought to play a key role on past atmospheric $CO_2$ variations. Here, we demonstrate that periods of high precession are coincident with anomalous $CO_2$ outgassing from the Southern Ocean. Under high precession, we find a poleward shift in the southern westerly winds, enhanced Southern Ocean meridional overturning, and an increase in the surface ocean partial pressure of $CO_2$ along the core of the Antarctic Circumpolar Current. These results suggest that orbital precession may have played an important role in driving changes in atmospheric $CO_2$.

**Plain Language Summary** Over the past one million years, Earth has experienced several glacial and interglacial periods. As a glacial period is ending, carbon in the atmosphere can rise by up to 50%. The cause for this change is currently unknown, but most theories suggest that this carbon is released from the deep ocean into the atmosphere. The Southern Ocean surrounding Antarctica is the location of a lot of carbon outgassing from the deep ocean into the atmosphere, so it could be responsible for some of this change in atmospheric carbon. One of Earth's orbital cycles, precession, has been shown to change circulation in the Southern Ocean, that can affect how much carbon is carried from the deep ocean to the surface and released into the atmosphere. This paper uses simulations of a climate model to show that high precession corresponds to a 20% increase in the release of carbon from the Southern Ocean into the atmosphere. These findings suggest that precession could have affected changes in past atmospheric carbon concentrations.

## 1. Introduction

The Southern Ocean plays a central role in the global carbon cycle (Marshall & Speer, 2012). The Southern Westerly Winds (SWW) interact with the ocean surface and force a zonally unbound meridional overturning circulation via Ekman transport, also known as the Upper Cell (Speer et al., 2000). On the poleward edge of this meridional overturning, deep, carbon-rich water is upwelled to the surface, and $CO_2$ is released into the atmosphere. Past studies have suggested that modern-day, interannual variability in the position and intensity of the SWW can invoke changes in Southern Ocean circulation, air-sea $CO_2$ flux, and atmospheric $CO_2$ concentration (Butler et al., 2007; Dufour et al., 2013; Landschützer et al., 2019; Lovenduski et al., 2007; Nevison et al., 2020), and can influence the global carbon cycle (Hauck et al., 2020).

The Southern Ocean likely played a key role in driving the large variations of atmospheric $CO_2$ observed over glacial-interglacial cycles (Anderson et al., 2009; Sigman et al., 2004; Toggweiler et al., 2006). This is because the Southern Ocean is one of the only places in the global ocean where dense ocean isopycnal surfaces outcrop, providing a means to connect the deep ocean interior to the atmosphere (Rintoul et al., 2001). However, the mechanisms responsible for changing air-sea $CO_2$ flux in the Southern Ocean on these timescales are not fully understood. In line with results from studies of modern-day Southern Ocean $CO_2$ flux variability, multiple manuscripts suggest that glacial-interglacial changes in the SWW may have played a role in some of these changes in air-sea $CO_2$ flux (Anderson et al., 2009; Ai et al., 2020; d'Orgeville et al., 2010; Lee et al., 2011; Menviel et al., 2008; Toggweiler et al., 2006; Tschumi et al., 2008). In these studies, the authors invoke SWW changes via mechanisms such as a global temperature increase (Toggweiler et al., 2006), a cooling North Atlantic (Anderson et al., 2009; Lee et al., 2011), or variations in Earth's axial tilt (obliquity) (Ai et al., 2020), yet no clear consensus on the cause of the SWW changes has emerged.

Recent studies suggest that the climate in the high-latitude Southern Hemisphere responds to orbital precession, one of the Milankovitch cycles with a spectral peak at ∼21,000 years. Orbital precession increases the seasonal cycle of insolation over one hemisphere while decreasing the magnitude of the seasonal cycle in the opposite hemisphere; this is especially pronounced at high latitudes. Modeling and proxy studies have demonstrated that precession can significantly alter the position and strength of the SWW, which impacts circulation in the Southern Ocean (Lamy et al., 2019; Rutberg & Broccoli, 2019). Yet the models used in these studies are lacking a carbon cycle and thus are unable to predict if Southern Ocean air-sea $CO_2$ flux will be affected by precession.

Here, we use a state-of-the-art Earth system model which includes a representation of the carbon cycle to illustrate, for the first time, that orbital precession can have a marked impact on Southern Ocean air-sea $CO_2$ flux. We compare output from two simulations with different precessional states to illustrate the potential influence of precession on the Southern Ocean. As we will demonstrate, precession drives changes in the SWW and Southern Ocean circulation, alters the upwelling of deep, carbon-rich water, and produces anomalies in air-sea $CO_2$ flux. Our results suggest that orbital precession plays an important role in regulating atmospheric $CO_2$ concentrations, and provide a possible mechanism to explain the precessional peak in the ice core atmospheric $CO_2$ spectra.

## 2. Methods

Our primary numerical modeling tool is the low-resolution configuration of the Community Earth System Model (CESM) version 2.1.1 (Danabasoglu et al., 2020), a fully coupled climate model designed for long climate integrations (Shields et al., 2012). The atmospheric component, CAM4, has a resolution of ∼3.75° × 3.75° and 26 vertical levels (Neale et al., 2013). The ocean component, POP2, has nominal 2° latitude × 4° longitude resolution (lowering to less than 2° latitude resolution in the Southern Ocean), and 60 vertical levels (Danabasoglu et al., 2012; Smith et al., 2010). POP2 represents subgrid-scale processes, such as mesoscale and submesoscale processes, via a collection of parameterizations (Danabasoglu et al., 2008). Importantly, the Gent and Mcwilliams (1990) mesoscale eddy parameterization includes a variable eddy-induced advection coefficient (Gent, 2016) which improves realism of eddy-driven mixing of carbon in the Southern Ocean at coarse resolution (Lovenduski et al., 2013). POP2 includes a biogeochemical model, MARBL (Long et al., 2021). MARBL contains multiple chemical tracers necessary for simulating ocean biogeochemistry such as carbon, nitrogen, phosphorus, iron, silicon, and oxygen.

Our experiment was designed to isolate the impact of precession on the Southern Ocean. We spun up CESM 2.1.1 for a 1000-year period with an eccentricity parameter of 0; since eccentricity modulates the strength of precession, this equilibration period had no precessional forcing. Carbon dioxide in the atmosphere is kept at a constant preindustrial value of 284.7 ppm. Over the last 500 years of the spinup, the globally integrated air-sea $CO_2$ flux drift is negligible ($-1.9 \pm 6.5 \times 10^{-6}$ Pg C yr$^{-2}$; Figure S2 in Supporting Information S1). Following the spin-up period, two 100-year simulations were performed: the first, NoPrec, maintains an eccentricity parameter of 0, while the second, HighPrec, uses an eccentricity parameter of 0.058, which is the maximum value over the last one million years (Laskar et al., 2004). A high value of eccentricity was chosen to maximize the precessional signal in HighPrec. Because the eccentricty parameter was kept as zero in NoPrec, there is no precessional impact on insolation (Figure S1a in Supporting Information S1). In the HighPrec simulation, the Southern Hemisphere summer solstice was configured to occur at the perihelion of Earth's orbit, which maximizes seasonal variability of insolation in the Southern Hemisphere (Figure S1b in Supporting Information S1). A full depiction of the differences in insolation between HighPrec and NoPrec is shown in Figure S1c in Supporting Information S1. We are confident in using 100-year means to study changes in the Southern Ocean because our HighPrec simulation illustrates an immediate response of SWW, despite a minimal drift in global mean surface temperature. This result is consistent with the expectation of a negligible impact of precession on annual mean insolation. Both HighPrec and NoPrec show minimal drift in globally integrated air-sea $CO_2$ flux over the 100 years studied; NoPrec has a global drift of $0.4 \pm 5.3 \times 10^{-4}$ Pg C yr$^{-2}$ and HighPrec has a global drift of $3.2 \pm 4.5 \times 10^{-4}$ Pg C yr$^{-2}$.

While CESM2 is a well-validated model (Danabasoglu et al., 2020; Long et al., 2021; Simpson et al., 2020), here we employ CESM2 components with lower resolution than the standard configuration, requiring an assessment of model validity at this resolution. Of particular interest in this study is the position and strength of the SWW. While the maximum zonal wind stress in the NoPrec SWW (0.14 N m$^{-2}$) agrees with modern estimates (Large & Yeager, 2009, 0.14 N m$^{-2}$), the modeled position of the SWW zonal wind stress (centered on 45°S) shows an equatorward bias relative to the estimated preindustrial value (Large & Yeager, 2009, centered on 53°S), which

is a consequence of the lower resolution of the atmospheric model (Shields et al., 2012). The modeled position and strength of the SWW in our NoPrec simulation is within the range reported by models that participated in the Palaeoclimate Model Intercomparison Projects PMIP2 and PMIP3 under preindustrial conditions (Rojas, 2013), whose model components are simulated at a similar resolution as in our experiment. We find that the version of CESM2 employed in this study captures the air-sea fluxes of pre-industrial/natural $CO_2$ as compared to an observation-based inversion, as biome-mean $CO_2$ fluxes over the last 500 years of the spin-up simulation are within the uncertainty of the observation-based fluxes (Mikaloff Fletcher et al., 2007) (Table S1 in Supporting Information S1).

A goal of this study is to isolate the different physical processes driving changes in air-sea $CO_2$ flux over the Southern Ocean. We approach this using the air-sea $CO_2$ flux equation as solved by the model:

$$F_{CO_2} = k_{sol} \times A_{noice} \times \Delta pCO_2 \times k_{gtv}, \tag{1}$$

where $k_{sol}$ is the solubility of carbon in seawater, $A_{noice}$ is the surface area without ice, $\Delta pCO_2$ is the difference in the partial pressure of $CO_2$ between the surface ocean and the atmosphere, and $k_{gtv}$ is the gas transfer velocity which is driven by surface winds (Wanninkhof, 2014; Wanninkhof et al., 2013). We isolate the contribution from each process as follows:

$$\delta[F]_{k_{sol}} = \delta[k_{sol}] \times A_{noice} \times \Delta pCO_2 \times k_{gtv}, \tag{2}$$

where $\delta[F]_{k_{sol}}$ is used to quantify the impact of precession-driven changes in solubility $(\delta k_{sol})$ on air-sea $CO_2$ flux. The $\delta$ symbol corresponds to the algebraic difference between the HighPrec and NoPrec value of the designated variable, and the non-$\delta$ terms are taken directly from the NoPrec simulation.

We expanded this technique to include effects from changes in the covariance among the terms in Equation 1. Only one of these terms, the combination of $\Delta pCO_2$ and $k_{gtv}$, was significant relative to the changes computed using Equation 2. The influence of joint changes in these two processes was calculated as follows:

$$\delta[F]_{\Delta pCO_2, k_{gtv}} = k_{sol} \times A_{noice} \times \delta[\Delta pCO_2] \times \delta[k_{gtv}], \tag{3}$$

which isolates the impact of simultaneous, precession-driven changes in both $\Delta pCO_2$ and $k_{gtv}$. It is important to note that since $CO_2$ in the atmosphere is kept constant, the $\Delta pCO_2$ term in the air-sea $CO_2$ flux decomposition corresponds to only changes in surface ocean $pCO_2$. In this analysis, it also became important to distinguish between the different variables controlling surface ocean $pCO_2$. Because $pCO_2$ is not calculated in CESM with a simple equation as in air-sea $CO_2$ flux (Equation 1), this decomposition was instead performed using a first order Taylor Expansion. Contributions from temperature, salinity, Dissolved Inorganic Carbon (DIC), alkalinity, and freshwater forcing are distinguished in their effects on surface ocean $pCO_2$ (see Appendix A of Lovenduski et al., 2007).

In this manuscript, we emphasize orbital precession-driven changes in the Southern Ocean, calculated as the difference between the century-mean values in the 100-year HighPrec simulation and the 100-year NoPrec simulation. This difference is only reported to be statistically significant if it surpasses the 99% confidence level (Text S1 in Supporting Information S1).

## 3. Results

Our simulations show that high precession produces a shift in the SWW that manifests most strongly in the austral summer relative to conditions with no precessional forcing. In the summer months (DJF), we find a $\sim$6 m s$^{-1}$ increase in the zonal-mean wind speed extending from 300 to 100 hPa and centered at 50°S; we also find a $\sim$3 m s$^{-1}$ decrease at the same heights centered on 30°S (Figure 1b). Whereas, in the winter months (JJA), high precession leads to a general weakening of the SWW in JJA (Figure 1c). The shift in the SWW during the DJF season exceeds the SWW weakening in the JJA season, resulting in an annual mean shift (Figure 1a). This poleward shift in the SWW appears throughout the entire vertical structure of the atmosphere, indicating a poleward intensification of the surface westerlies that drive Southern Ocean circulation.

The simulated precessional shift in the SWW corresponds to large deviations in the atmospheric temperature structure. We find that the strongest temperature anomalies occur during the DJF season, due to austral summer
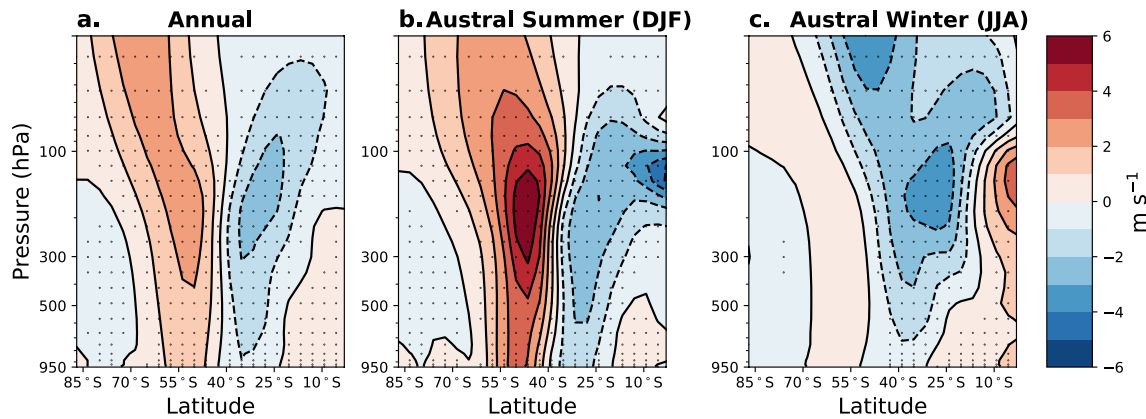
**Figure 1.** Precession-driven anomalies in Southern Hemisphere zonal-mean wind speed (m s$^{-1}$), calculated as the century-mean difference from the HighPrec and NoPrec simulations. (a) Annual-mean anomalies, (b) Austral summer (DJF) anomalies, and (c) Austral winter (JJA) anomalies. Stippling indicates a statistically significant difference at the 99% confidence level (Text S1 in Supporting Information S1). Positive values/contours correspond to westerly wind anomalies.

receiving significantly more insolation in periods of high precession (Figure S3 in Supporting Information S1). We find a precession-driven increase in the pole-to-Equator temperature gradient around 200 hPa in both the annual-mean and DJF zonal-mean temperature profiles (Figures S3g and S3h in Supporting Information S1) that corresponds to the greatest wind anomalies (Figures 1a and 1b). These findings indicate that periods of high precession, or periods when the perihelion of Earth's orbit occur at the Southern Hemisphere summer solstice, are associated with an enhanced pole-to-Equator temperature gradient at the approximate position of the tropopause.

Carbon outgassing in the Southern Ocean increases by approximately 20% in HighPrec relative to NoPrec. The century-mean, integrated (<35°S) air-sea $CO_2$ flux increases from 0.264 ± 0.013 Pg C yr$^{-1}$ in NoPrec to 0.322 ± 0.014 Pg C yr$^{-1}$ in HighPrec. The null hypothesis that these values are the same can be rejected with a 99% confidence level, and the uncertainty values reported here represent the standard error of the mean (Text S1 in Supporting Information S1). This precession-driven anomalous air-sea $CO_2$ flux is most pronounced in the Indian and Pacific sectors of the Southern Ocean: regions typically characterized by outgassing or weak uptake of $CO_2$ (Figure 2c). North of the ACC streamlines, and in the Atlantic sector of the ACC, high precession is associated with anomalous uptake of $CO_2$ (Figure 2). Differences in air-sea $CO_2$ flux between HighPrec and NoPrec change depending on the season, and the greatest increases in carbon outgassing are found in austral summer and austral autumn (Figure S4 in Supporting Information S1). The precession-driven anomalous outgassing exceeds the anomalous uptake, such that the Southern Ocean becomes a larger net source of $CO_2$ to the atmosphere under high precession relative to no precession.
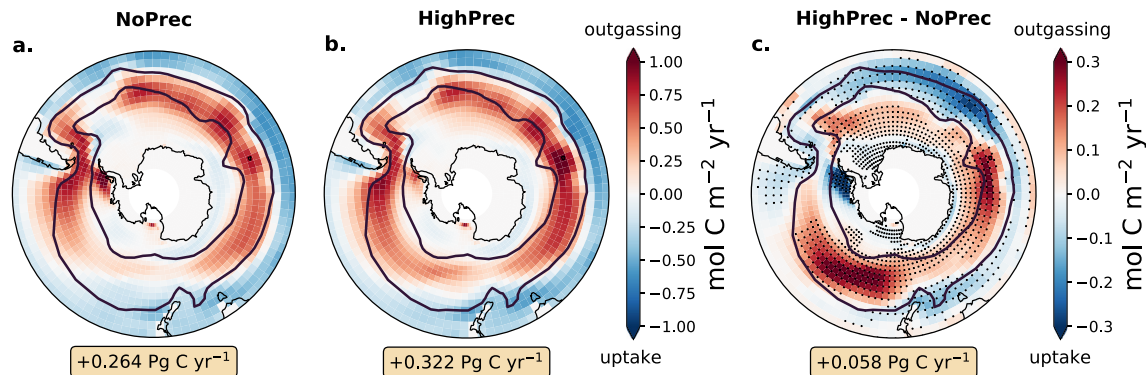


**Figure 2.** (a) Century-mean sea-air $CO_2$ flux from the NoPrec simulation. (b) Century-mean sea-air $CO_2$ flux from the HighPrec simulation. (c) Precession-driven change in sea-air $CO_2$ flux, calculated as the difference in century-mean $CO_2$ flux from the HighPrec and NoPrec simulations. Stippling indicates a statistically significant difference at the 99% confidence level (Text S1 in Supporting Information S1). Units are mol C m$^{-2}$ yr$^{-1}$, and positive values correspond to $CO_2$ outgassing. Black lines show the Antarctic Circumpolar Current (ACC) in the NoPrec simulation, bound by the 7 and 100 Sv barotropic streamlines. Numbers under each map indicate the Southern Ocean (<35°S) integrated flux and anomalous flux, respectively (Pg C yr$^{-1}$).
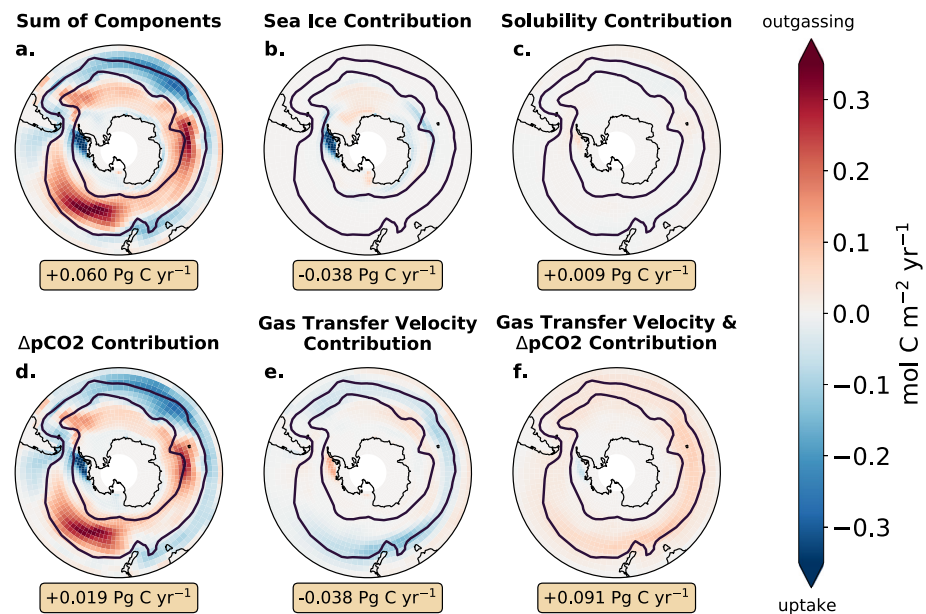
**Figure 3.** Contribution of (b) sea ice extent, (c) solubility, (d) $\Delta pCO_2$, (e) gas transfer velocity, and (f) the combination of gas transfer velocity and $\Delta pCO_2$ change to the total air-sea $CO_2$ flux difference (mol C m$^{-2}$ yr$^{-1}$) due to precession. Contributions calculated as in Equation 2 and Equation 3 using the century-mean differences in each variable from the HighPrec and NoPrec simulations. (a) Shows the sum of the five components (b–f), which is nearly identical to Figure 2. Black lines show the Antarctic Circumpolar Current (ACC) in the NoPrec simulation, bound by the 7 and 100 Sv barotropic streamlines. Numbers under each map indicate the Southern Ocean (<35°S) integrated contribution to the anomalous flux (Pg C yr$^{-1}$).

The precession-driven increase in Southern Ocean sea-air $CO_2$ flux is a result of changes in both surface ocean $pCO_2$ and the gas transfer velocity caused by changes in precession. We isolated the influence of each physical process driving changes in air-sea flux using the technique outlined in Methods. We find that the spatial pattern of the changes in $CO_2$ flux is driven by the contribution from $\Delta pCO_2$ (determined by surface ocean $pCO_2$ since carbon in the atmosphere is constant) (Figure 3), which itself is impacted by changing surface ocean DIC (Figure S5 in Supporting Information S1). This indicates that the surface ocean $pCO_2$ response to precession drives the anomalous outgassing in the Indian and Pacific sectors of the ACC and the anomalous uptake in the Atlantic sector of the ACC. Because of the strong correlation between surface ocean DIC and surface $pCO_2$ (Figure S5e in Supporting Information S1e), we can attribute the majority of these changes to an altered ocean circulation. When integrated over the Southern Ocean (<35°S), the large magnitude positive and negative $\Delta pCO_2$ anomalies nearly balance, such that the net contribution to the integrated flux difference is small (0.019 Pg C yr$^{-1}$; Figure 3d). The precession-driven $CO_2$ flux difference is also strongly affected by the simultaneous changes in the gas transfer velocity and $\Delta pCO_2$, which contribute to enhanced outgassing in the ACC and a large, positive Southern Ocean integrated flux contribution (0.091 Pg C yr$^{-1}$; Figure 3f). The changes in gas transfer velocity contributes a moderate decrease in carbon outgassing of $-0.038$ Pg C yr$^{-1}$ (Figure 3e). Whereas, the changes in air-sea $CO_2$ flux due to sea ice extent (Figure 3b) and solubility (Figure 3c) have minimal impacts on the flux difference, with the exception of sea ice extent near the West Antarctic Peninsula which drives localized anomalous $CO_2$ uptake (Figure 3b).

The core of the Southern Ocean meridional overturning circulation shifts poleward and deepens under high precession, tapping into a richer carbon source explaining the increase in surface $pCO_2$. Relative to the NoPrec simulation, both the wind stress and overturning maxima shift southward by ~1° in the HighPrec simulation (Figure 4). In its more poleward position, the meridional overturning circulation streamlines intersect waters with higher DIC concentrations (Figure 4b). For example, the 20 Sv streamline in the NoPrec simulation intersects waters only up to 1,250 m deep with maximum DIC concentrations of ~2,330 mmol m$^{-3}$. In contrast, this streamline reaches a deeper depth of 1,500 m in the HighPrec simulation overlapping with higher DIC concentration of ~2,340 mmol m$^{-3}$ (Figure 4). This shifted and deepened meridional overturning increases the amount of carbon that is brought to the surface in HighPrec relative to NoPrec, which is a key component (Figure S5 in Supporting Information S1) of the simulated increase in $CO_2$ outgassing.
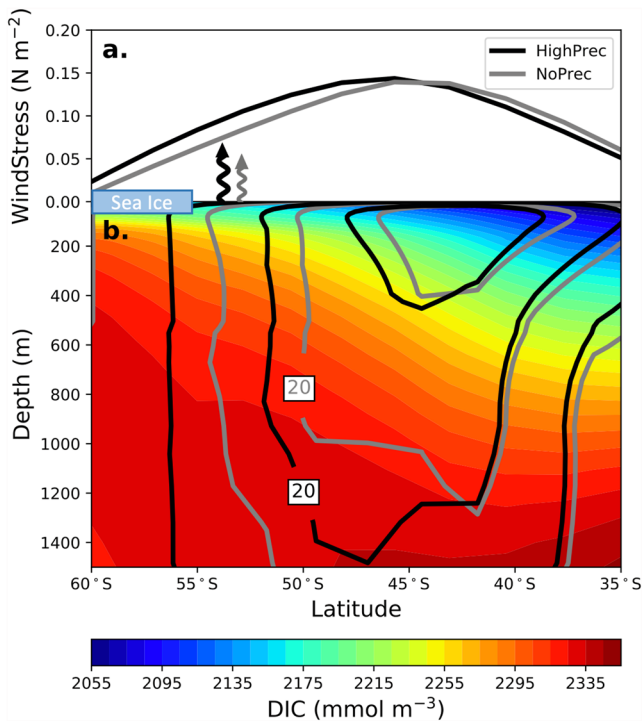
**Figure 4.** Southern Ocean response to high precession. (a) Century-mean zonal-mean surface wind stress from (gray) the NoPrec simulation and (black) the HighPrec simulation. (b) Century-mean (colors) zonal-mean DIC concentration from the HighPrec simulation with meridional overturning streamlines from the (gray) NoPrec simulation and (black) HighPrec simulation. Overturning units are Sv with contour lines every 10 Sv; positive streamlines indicate clockwise flow. Squiggly arrows indicate the relative position and strength in the annual peak carbon outgassing in both simulations.

The largest increases in air-sea $CO_2$ flux occur where precession drives both enhanced gas exchange velocities and anomalous meridional and vertical advection of carbon-rich water (Figures 2–4, and Figure S6 in Supporting Information S1). High precession is associated with increases in the modeled air-sea gas transfer velocity, $k_{gtv}$, near the northern core of the ACC; these increases are especially pronounced in the Indian and western Pacific sectors (Figure S6b in Supporting Information S1). The SWW changes that induce increases in near surface turbulence and air-sea gas exchange also alter the ocean circulation (Figure 4), driving increases in surface ocean DIC and $pCO_2$ in the Indian and western Pacific sectors of the ACC (Figures S6b and S5a in Supporting Information S1). Where the gas transfer velocity and $pCO_2$ anomalies align, they combine to produce enhanced $CO_2$ outgassing (Figures 2b and 4).

## 4. Conclusions and Discussion

Our study demonstrates that high precessional states impact key Southern Ocean processes involved in the global carbon cycle, ultimately leading to a substantial increase in sea-air $CO_2$ flux. Under high precessional forcing of the Southern Hemisphere, our model predicts a ∼1° poleward shift of the SWW across the troposphere, likely caused by insolation-driven atmospheric temperature changes over Antarctica. The associated poleward shift in the SWW drives a stronger and deeper meridional overturning circulation, enhancing the vertical and lateral advection of carbon-rich water. The shifted SWW also increase turbulent air-sea exchange which combined with the changes ocean overturning combine to produce a 20% increase in $CO_2$ outgassing from the Southern Ocean.

The precession-driven poleward shift in the SWW predicted by our model strongly resembles a positive phase of the Southern Annular Mode (SAM; see, e.g., Figure 7 of Thompson et al., 2000), albeit with a different seasonality. While the SAM pattern has been linked to internal climate variability and anthropogenic forcing, here we demonstrate that the Southern Hemisphere seasonal insolation changes associated with precession produce a similar shift in the SWW. The simulated change in the equator-to-pole temperature gradient in the upper troposphere is similar to that of the positive SAM phase, when the polar atmosphere shows cooling aloft associated with Ozone forcing (see Figure 8 of Thompson et al., 2000). Periods of high precession shift and deepen the meridional overturning circulation in our model (Figure 4b), which has also been found to occur during positive phases of the SAM (Yang et al., 2007). Thus, results from our simulations suggest that the Southern Hemisphere response to precessional forcing exhibits similar features to the Southern Hemisphere response to variability associated with the SAM, suggesting that past changes could be used to understand ongoing changes in Southern Hemisphere climate.

The precession-driven changes in ocean meridional overturning and air-sea $CO_2$ flux that we report somewhat agrees with other modeling studies that have tested similar relationships. These studies impose direct changes to the SWWs by strength, position, or both and measure the resulting changes in atmospheric $CO_2$ concentrations (d'Orgeville et al., 2010; Menviel et al., 2008; Tschumi et al., 2008). In Menviel et al. (2008), a positive relationship is found between SWW strength and carbon outgassing in the Southern Ocean. In addition, the modeling studies performed in Tschumi et al. (2008) find a positive relationship between the strength of the SWWs and global atmospheric $CO_2$ concentrations. However, Tschumi et al. (2008) also finds that a poleward shift in the SWWs reduces the amount of atmospheric $CO_2$. This is attributed to a reduction in the area of outcropping deep water in the Southern Ocean. This disagrees with the results presented here. While it is difficult to diagnose the reason for this difference, it is likely because the changes in the SWWs between HighPrec and NoPrec have variance in both seasonal (Figure 1) and spatial (Figure S6a in Supporting Information S1) structure. This is because the SWW change in this study is due to precessional changes, not imposed directly. This disagreement may also be due to a difference in ocean models; Tschumi et al. (2008) uses the Bern3D which is a frictional-geostrophic

balance ocean model (Edwards & Marsh, 2005; Müller et al., 2006). Finally, d'Orgeville et al. (2010) suggests that a poleward shift in SWWs result in an increase of Southern-Ocean carbon outgassing, which agrees with the results presented here.

Our study uses an Earth system model that is configured with relatively coarse horizontal resolution in the atmosphere and ocean model components to support long integrations potentially affect the realism of our results. The average annual peak in zonal-mean wind stress occurs at 45°S in our model. While this shows good agreement with other models that have similar horizontal resolution (see Figure 3 of Shields et al., 2012), this position is equatorward relative to the modern-day position of 53° Large and Yeager (2009). Similar poleward shift in the position of the SWW in response to high precession is also found in other modeling studies with higher resolution, suggesting our results are not model dependent For instance, Rutberg and Broccoli (2019) used a model with a resolution of 2° latitude by 2.5° longitude in the atmosphere and found a poleward shift of 4° between extreme precessional states. The coarse resolution of our ocean model component requires that processes influenced by mesoscale eddies are parameterized. Numerous studies have emphasized the importance of mesoscale eddies in Southern Ocean meridional overturning, especially in its response to changes in surface wind stress (Abernathey et al., 2011; Doddridge et al., 2019; Hallberg & Gnanadesikan, 2006; Marshall & Radko, 2003; Marshall & Speer, 2012). Our model uses a variable eddy-induced advection coefficient (Gent, 2016), which has been shown to capture the sensitivity of these unresolved processes to changes in circulation (Lovenduski et al., 2013). Indeed, results from our model indicate that the eddy-induced meridional overturning circulation strengthens in response to SWW changes under high precession (counterclockwise anomalies in Figure S7b in Supporting Information S1), suggesting that our coarse resolution ocean model component is capable of capturing changes in unresolved eddy advection. However, there are studies that suggest that this response is model dependent and would likely alter the circulation response seen here (Bishop et al., 2016; Böning et al., 2008; Meredith et al., 2012; Tesdal et al., 2023). Future work should explore the responses identified here using a higher resolution configuration of capable of resolving these processes.

Taken together, our findings imply that orbital precession plays an important role in regulating atmospheric carbon dioxide concentration through its effect on the Southern Ocean. The present study is focused on the impact of precession on Southern Ocean $CO_2$ fluxes; however, it is likely that other regions could be similarly affected by changes in precession. While this analysis stems from the results of a single model, individual components of the dynamical mechanisms presented here have been described in prior studies using diverse sources of simulations, paleo-proxy evidence, and instrumental observations (Butler et al., 2007; Dufour et al., 2013; Lamy et al., 2019; Lovenduski et al., 2007; Nevison et al., 2020; Rutberg & Broccoli, 2019). As we have demonstrated, the changes in seasonal insolation associated with orbital precession could have driven to a shift in the position of the westerly winds over the Southern Ocean, increasing the upwelling of carbon-rich water to the surface exchanging more carbon with the atmosphere. This mechanism could explain variability in ice core records of atmospheric $CO_2$ variability on precessional timescales (Petit et al., 1999).

## Data Availability Statement

The analysis data of the CESM simulation in this study were uploaded to https://doi.org/10.5281/zenodo.7761019.

## References

Abernathey, R., Marshall, J., & Ferreira, D. (2011). The dependence of southern ocean meridional overturning on wind stress. *Journal of Physical Oceanography*, *41*(12), 2261–2278. https://doi.org/10.1175/jpo-d-11-023.1

Ai, X. E., Studer, A. S., Sigman, D. M., Martínez-García, A., Fripiat, F., Thöle, L. M., et al. (2020). Southern ocean upwelling, earth's obliquity, and glacial-interglacial atmospheric $CO_2$ change. *Science*, *370*(6522), 1348–1352. https://doi.org/10.1126/science.abd2115

Anderson, R., Ali, S., Bradtmiller, L., Nielsen, S., Fleisher, M., Anderson, B., & Burckle, L. (2009). Wind-driven upwelling in the southern ocean and the deglacial rise in atmospheric $CO_2$. *Science*, *323*(5920), 1443–1448. https://doi.org/10.1126/science.1167441

Bishop, S. P., Gent, P. R., Bryan, F. O., Thompson, A. F., Long, M. C., & Abernathey, R. (2016). Southern ocean overturning compensation in an eddy-resolving climate simulation. *Journal of Physical Oceanography*, *46*(5), 1575–1592. https://doi.org/10.1175/jpo-d-15-0177.1

Böning, C. W., Dispert, A., Visbeck, M., Rintoul, S., & Schwarzkopf, F. U. (2008). The response of the Antarctic circumpolar current to recent climate change. *Nature Geoscience*, *1*(12), 864–869. https://doi.org/10.1038/ngeo362

Butler, A. H., Thompson, D. W., & Gurney, K. R. (2007). Observed relationships between the southern annular mode and atmospheric carbon dioxide. *Global Biogeochemical Cycles*, *21*(4), GB4014. https://doi.org/10.1029/2006gb002796

Danabasoglu, G., Bates, S. C., Briegleb, B. P., Jayne, S. R., Jochum, M., Large, W. G., et al. (2012). The CCSM4 ocean component. *Journal of Climate*, *25*(5), 1361–1389. https://doi.org/10.1175/jcli-d-11-00091.1

Danabasoglu, G., Ferrari, R., & McWilliams, J. C. (2008). Sensitivity of an ocean general circulation model to a parameterization of near-surface eddy fluxes. *Journal of Climate*, *21*(6), 1192–1208. https://doi.org/10.1175/2007jcli1508.1

Danabasoglu, G., Lamarque, J.-F., Bacmeister, J., Bailey, D., DuVivier, A., Edwards, J., et al. (2020). The community Earth system model version 2 (CESM2). *Journal of Advances in Modeling Earth Systems*, *12*(2), e2019MS001916. https://doi.org/10.1029/2019ms001916

Doddridge, E. W., Marshall, J., Song, H., Campin, J.-M., Kelley, M., & Nazarenko, L. (2019). Eddy compensation dampens southern ocean sea surface temperature response to westerly wind trends. *Geophysical Research Letters*, *46*(8), 4365–4377. https://doi.org/10.1029/2019gl082758

d'Orgeville, M., Sijp, W., England, M., & Meissner, K. (2010). On the control of glacial-interglacial atmospheric $CO_2$ variations by the southern hemisphere westerlies. *Geophysical Research Letters*, *37*(21), L21703. https://doi.org/10.1029/2010gl045261

Dufour, C. O., Sommer, J. L., Gehlen, M., Orr, J. C., Molines, J.-m., Simeon, J., & Barnier, B. (2013). Eddy compensation and controls of the enhanced sea-to-air $CO_2$ flux during positive phases of the southern annular mode. *Global Biogeochemical Cycles*, *27*(3), 950–961. https://doi.org/10.1002/gbc.20090

Edwards, N. R., & Marsh, R. (2005). Uncertainties due to transport-parameter sensitivity in an efficient 3-D ocean-climate model. *Climate Dynamics*, *24*(4), 415–433. https://doi.org/10.1007/s00382-004-0508-8

Gent, P. R. (2016). Effects of southern hemisphere wind changes on the meridional overturning circulation in ocean models. *Annual Review of Marine Science*, *8*(1), 79–94. https://doi.org/10.1146/annurev-marine-122414-033929

Gent, P. R., & Mcwilliams, J. C. (1990). Isopycnal mixing in ocean circulation models. *Journal of Physical Oceanography*, *20*(1), 150–155. https://doi.org/10.1175/1520-0485(1990)020<0150:imiocm>2.0.co;2

Hallberg, R., & Gnanadesikan, A. (2006). The role of eddies in determining the structure and response of the wind-driven southern hemisphere overturning: Results from the modeling eddies in the southern ocean (MESO) project. *Journal of Physical Oceanography*, *36*(12), 2232–2252. https://doi.org/10.1175/jpo2980.1

Hauck, J., Zeising, M., Le Quéré, C., Gruber, N., Bakker, D. C., Bopp, L., et al. (2020). Consistency and challenges in the ocean carbon sink estimate for the global carbon budget. *Frontiers in Marine Science*, *7*, 571720. https://doi.org/10.3389/fmars.2020.571720

Lamy, F., Chiang, J. C., Martínez-Méndez, G., Thierens, M., Arz, H. W., Bosmans, J., et al. (2019). Precession modulation of the south pacific westerly wind belt over the past million years. *Proceedings of the National Academy of Sciences of the United States of America*, *116*(47), 23455–23460. https://doi.org/10.1073/pnas.1905847116

Landschützer, P., Ilyina, T., & Lovenduski, N. S. (2019). Detecting regional modes of variability in observation-based surface ocean $pCO_2$. *Geophysical Research Letters*, *46*(5), 2670–2679. https://doi.org/10.1029/2018gl081756

Large, W., & Yeager, S. (2009). The global climatology of an interannually varying air–sea flux data set. *Climate Dynamics*, *33*(2–3), 341–364. https://doi.org/10.1007/s00382-008-0441-3

Laskar, J., Robutel, P., Joutel, F., Gastineau, M., Correia, A., & Levrard, B. (2004). A long-term numerical solution for the insolation quantities of the earth. *Astronomy & Astrophysics*, *428*(1), 261–285. https://doi.org/10.1051/0004-6361:20041335

Lee, S.-Y., Chiang, J. C., Matsumoto, K., & Tokos, K. S. (2011). Southern ocean wind response to north Atlantic cooling and the rise in atmospheric $CO_2$: Modeling perspective and paleoceanographic implications. *Paleoceanography*, *26*(1), PA1214. https://doi.org/10.1029/2010pa002004

Long, M. C., Moore, J. K., Lindsay, K., Levy, M., Doney, S. C., Luo, J. Y., et al. (2021). Simulations with the marine biogeochemistry library (MARBL). *Journal of Advances in Modeling Earth Systems*, *13*(12), e2021MS002647. https://doi.org/10.1029/2021ms002647

Lovenduski, N. S., Gruber, N., Doney, S. C., & Lima, I. D. (2007). Enhanced $CO_2$ outgassing in the southern ocean from a positive phase of the southern annular mode. *Global Biogeochemical Cycles*, *21*(2), GB2026. https://doi.org/10.1029/2006gb002900

Lovenduski, N. S., Long, M. C., Gent, P. R., & Lindsay, K. (2013). Multi-decadal trends in the advection and mixing of natural carbon in the southern ocean. *Geophysical Research Letters*, *40*(1), 139–142. https://doi.org/10.1029/2012gl054483

Marshall, J., & Radko, T. (2003). Residual-mean solutions for the antarctic circumpolar current and its associated overturning circulation. *Journal of Physical Oceanography*, *33*(11), 2341–2354. https://doi.org/10.1175/1520-0485(2003)033<2341:rsftac>2.0.co;2

Marshall, J., & Speer, K. (2012). Closure of the meridional overturning circulation through southern ocean upwelling. *Nature Geoscience*, *5*(3), 171–180. https://doi.org/10.1038/ngeo1391

Menviel, L., Timmermann, A., Mouchet, A., & Timm, O. (2008). Climate and marine carbon cycle response to changes in the strength of the southern hemispheric westerlies. *Paleoceanography*, *23*(4), PA4201. https://doi.org/10.1029/2008pa001604

Meredith, M. P., Garabato, A. C. N., Hogg, A. M., & Farneti, R. (2012). Sensitivity of the overturning circulation in the southern ocean to decadal changes in wind forcing. *Journal of Climate*, *25*(1), 99–110. https://doi.org/10.1175/2011jcli4204.1

Mikaloff Fletcher, S., Gruber, N., Jacobson, A. R., Gloor, M., Doney, S., Dutkiewicz, S., et al. (2007). Inverse estimates of the oceanic sources and sinks of natural $CO_2$ and the implied oceanic carbon transport. *Global Biogeochemical Cycles*, *21*(1), GB1010. https://doi.org/10.1029/2006gb002751

Müller, S., Joos, F., Edwards, N., & Stocker, T. (2006). Water mass distribution and ventilation time scales in a cost-efficient, three-dimensional ocean model. *Journal of Climate*, *19*(21), 5479–5499. https://doi.org/10.1175/jcli3911.1

Neale, R. B., Richter, J., Park, S., Lauritzen, P. H., Vavrus, S. J., Rasch, P. J., & Zhang, M. (2013). The mean climate of the community atmosphere model (CAM4) in forced SST and fully coupled experiments. *Journal of Climate*, *26*(14), 5150–5168. https://doi.org/10.1175/jcli-d-12-00236.1

Nevison, C. D., Munro, D. R., Lovenduski, N. S., Keeling, R. F., Manizza, M., Morgan, E. J., & Rödenbeck, C. (2020). Southern annular mode influence on wintertime ventilation of the southern ocean detected in atmospheric $O_2$ and $CO_2$ measurements. *Geophysical Research Letters*, *47*(4), e2019GL085667. https://doi.org/10.1029/2019gl085667

Petit, J.-R., Jouzel, J., Raynaud, D., Barkov, N. I., Barnola, J.-M., Basile, I., et al. (1999). Climate and atmospheric history of the past 420,000 years from the Vostok ice core, Antarctica. *Nature*, *399*(6735), 429–436. https://doi.org/10.1038/20859

Rintoul, S. R., Hughes, C. W., & Olbers, D. (2001). The Antarctic circumpolar current system. In *International geophysics* (Vol. 77, pp. 271–XXXVI). Elsevier.

Rojas, M. (2013). Sensitivity of southern hemisphere circulation to LGM and 4×$CO_2$ climates. *Geophysical Research Letters*, *40*(5), 965–970. https://doi.org/10.1002/grl.50195

Rutberg, R., & Broccoli, A. (2019). Response of the high-latitude southern hemisphere to precessional forcing: Implications for pleistocene ocean circulation. *Paleoceanography and Paleoclimatology*, *34*(7), 1092–1106. https://doi.org/10.1029/2019pa003598

Shields, C. A., Bailey, D. A., Danabasoglu, G., Jochum, M., Kiehl, J. T., Levis, S., & Park, S. (2012). The low-resolution CCSM4. *Journal of Climate*, *25*(12), 3993–4014. https://doi.org/10.1175/jcli-d-11-00260.1

Sigman, D. M., Jaccard, S. L., & Haug, G. H. (2004). Polar ocean stratification in a cold climate. *Nature*, *428*(6978), 59–63. https://doi.org/10.1038/nature02357

Simpson, I. R., Bacmeister, J., Neale, R. B., Hannay, C., Gettelman, A., Garcia, R. R., et al. (2020). An evaluation of the large-scale atmospheric circulation and its variability in CESM2 and other CMIP models. *Journal of Geophysical Research: Atmospheres*, *125*(13), e2020JD032835. https://doi.org/10.1029/2020jd032835

Smith, R., Jones, P., Briegleb, B., Bryan, F., Danabasoglu, G., Dennis, J., et al. (2010). The parallel ocean program (POP) reference manual ocean component of the community climate system model (CCSM) and community earth system model (CESM). *LAUR-01853*, *141*, 1–140.

Speer, K., Rintoul, S. R., & Sloyan, B. (2000). The diabatic deacon cell. *Journal of Physical Oceanography*, *30*(12), 3212–3222. https://doi.org/10.1175/1520-0485(2000)030<3212:tddc>2.0.co;2

Tesdal, J.-E., MacGilchrist, G. A., Beadling, R. L., Griffies, S. M., Krasting, J. P., & Durack, P. J. (2023). Revisiting interior water mass responses to surface forcing changes and the subsequent effects on overturning in the southern ocean. *Journal of Geophysical Research: Oceans*, *128*(3), e2022JC019105. https://doi.org/10.1029/2022jc019105

Thompson, D. W., Wallace, J. M., & Hegerl, G. C. (2000). Annular modes in the extratropical circulation. Part II: Trends. *Journal of Climate*, *13*(5), 1018–1036. https://doi.org/10.1175/1520-0442(2000)013<1018:amitec>2.0.co;2

Toggweiler, J. R., Russell, J. L., & Carson, S. R. (2006). Midlatitude westerlies, atmospheric $CO_2$, and climate change during the ice ages. *Paleoceanography*, *21*(2), PA2005. https://doi.org/10.1029/2005pa001154

Tschumi, T., Joos, F., & Parekh, P. (2008). How important are southern hemisphere wind changes for low glacial carbon dioxide? A model study. *Paleoceanography*, *23*(4), PA4208. https://doi.org/10.1029/2008pa001592

Wanninkhof, R. (2014). Relationship between wind speed and gas exchange over the ocean revisited. *Limnology and Oceanography: Methods*, *12*(6), 351–362. https://doi.org/10.4319/lom.2014.12.351

Wanninkhof, R., Park, G.-H., Takahashi, T., Sweeney, C., Feely, R., Nojiri, Y., et al. (2013). Global ocean carbon uptake: Magnitude, variability and trends. *Biogeosciences*, *10*(3), 1983–2000. https://doi.org/10.5194/bg-10-1983-2013

Yang, X.-Y., Wang, D., Wang, J., & Huang, R. X. (2007). Connection between the decadal variability in the southern ocean circulation and the southern annular mode. *Geophysical Research Letters*, *34*(16), L16604. https://doi.org/10.1029/2007gl030526